

FRACTURE AND FATIGUE CRACK GROWTH FOR MICRO-SIZED SPECIMENS

K. Takashima and Y. Higo

Precision and Intelligence Laboratory, Tokyo Institute of Technology,
4259 Nagatsuta, Midori-ku, Yokohama 226-8503, Japan.

ABSTRACT

Fracture and fatigue tests were carried out on micro-sized specimens prepared from an electroless deposited Ni-P amorphous alloy thin film using a newly developed mechanical testing machine, and the size effects on the fracture and fatigue crack growth behavior have been discussed. Cantilever beam type specimens ($10 \times 12 \times 50 \mu\text{m}^3$) with notches were prepared from a Ni-P amorphous thin film by focused ion beam machining. Fatigue crack growth tests were carried out in air at room temperature under constant load amplitude using the testing machine for micro-sized specimens. Fatigue crack growth resistance curves were obtained from the measurement of striation spacing on the fatigue surface. Once fatigue crack growth occurs, the specimens failed after several thousand cycles. This indicates that the fatigue life of micro-sized specimens is mainly dominated by crack initiation. Fracture tests were performed for the specimens with fatigue pre-cracks ahead of the notches. The plane strain fracture toughness, K_{IC} , value was not obtained since the criteria of plane strain were not satisfied for this specimen size. As the plane strain requirements are determined by stress intensity and yield stress of the material, it is rather difficult for micro-sized specimens to satisfy these requirements. Plane stress and plane strain dominated regions were clearly observed on the fracture surfaces and their sizes were consistent with those estimated by fracture mechanics calculations. It is necessary to consider the results obtained in this investigation when designing actual MEMS devices.

KEYWORDS

Micro-sized specimen, MEMS, Fracture, Fatigue, Amorphous alloy, Thin film, Size effect

INTRODUCTION

Micro-sized machines and microelectromechanical systems (MEMS) are expected to be applied to bio-medical and micro-photonics devices such as micro-catheters for brain surgery and optical switches for electro-optical communications. The size of the components used in such MEMS devices is considered to be in the order of microns, and the mechanical properties of such micro-sized materials are considered to be different from those of bulk (ordinary sized) materials. Therefore, the evaluation of mechanical properties including elastic modulus, tensile strength, fracture toughness and fatigue properties are essential for practical applications of such MEMS devices. To date, there have been several studies which investigate the mechanical properties of small sized materials [1-3]. In particular, fracture toughness and fatigue crack growth properties of micro-sized materials are extremely important to enable reliable design of actual MEMS devices. In our previous studies, we have developed a new

type mechanical testing machine for micro-sized specimens, which can apply small amount of static and cyclic loads to the specimens [4, 5], and have obtained fatigue life curves of micro-sized Ni-P amorphous alloy specimens [6]. In addition to fatigue life, fatigue crack growth property and fracture toughness are also important for designing reliable and long-term durable MEMS devices. In this investigation, fracture and fatigue crack growth tests have been performed on Ni-P amorphous alloy micro-sized specimens, and the size effects on the fracture and fatigue crack growth behavior have been discussed.

EXPERIMENTAL PROCEDURE

Material and Specimen Preparation

The material used in this investigation was a Ni-11.5 mass%P amorphous thin film electroless plated on an Al-4.5 mass%Mg alloy. The thickness of the amorphous layer was 12 μm and that of the Al-4.5 mass%Mg alloy substrate was 0.79 mm, respectively. A disk with a diameter of 3 mm was cut from the Ni-P/Al-Mg sheet by electro discharge machining. An amorphous layer was separated from the Al-Mg alloy substrate by dissolving the substrate with a NaOH aqueous solution. The amorphous thin film was fixed on a holder and two types of micro-cantilever beam specimens with dimensions of 10 (B) \times 12 (W) \times 50 (L) μm^3 were cut from the amorphous layer by focused ion beam machining. This specimen size is equivalent to approximately 1/1000 of ordinary sized bending specimens. Figure 1 show a specimen prepared by the above procedures.

Testing Machine

Fatigue crack growth and fracture tests were carried out using a newly developed fatigue testing machine for micro-sized specimens. Figure 2 shows a block diagram of the fatigue testing machine. A magnetostrictive device is used as an actuator, which is able to produce displacements upto $\pm 10 \mu\text{m}$ with an accuracy of 5 nm, and the maximum response frequency of cyclic displacement is 100 Hz. The end of the actuator is connected to a metal shaft and a diamond tip of 5 μm in radius is attached to the other end of the shaft. The displacement of the actuator is measured by a laser displacement meter with an accuracy of 5 nm and the displacement signal is used as feed back control. The micro-sized specimen is set in a specimen holder and the holder is placed on a load cell as shown in Fig. 2. Small amount of displacement is applied to the specimen through the diamond tip. The amount of load applied to the specimen is measured by a strain gauge type load cell with a load resolution of 10 μN that is set under the specimen. The horizontal location of the specimen stage can be moved to adjust the loading position precisely by a stepping motor with a translation resolution of 0.1 μm . Further details of the testing machine are described in our previous papers [4, 5].

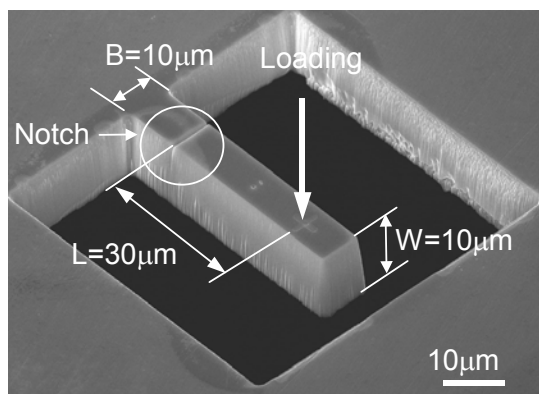


Figure 1: Scanning electron micrograph of micro-sized cantilever beam specimen prepared by focused ion beam machining.

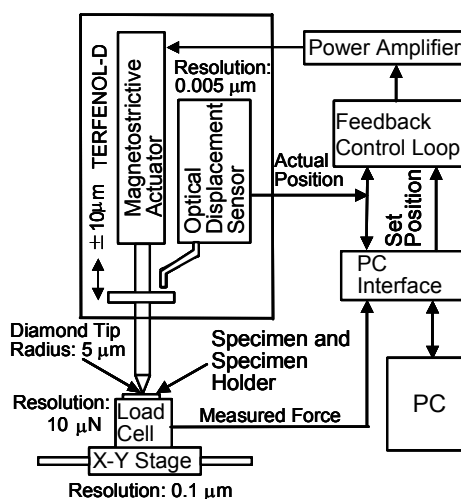


Figure 2: Block diagram of mechanical testing machine for micro-sized specimens.

Fatigue Test

In fatigue crack growth tests, notches with a depth of 3 μm were introduced into the specimens by focused ion beam machining. This notch depth is equivalent to $a/W = 0.25$, where a is notch length and W is specimen width. The width of the notch was 0.5 μm , and the notch radius is thus deduced to be 0.25 μm . The notch position was 10 μm from the fixed end of the specimen. The loading position is set at 40 μm from the fixed end of the specimen. Fatigue crack growth tests were performed in air at room temperature. Fatigue tests were carried out at a frequency of 10 Hz and a stress ratio, R ($R = P_{\min} / P_{\max}$, where P_{\min} is the minimum load and P_{\max} is the maximum load applied over the fatigue cycle) of 0.5 under constant load amplitude ($\Delta P/2$, where $\Delta P = P_{\max} - P_{\min}$) of 2 mN. Although the crack length was not able to be measured directly in this testing machine, the change in specimen compliance can be measured during fatigue tests. The initiation of crack growth was then determined by monitoring the specimen compliance.

Fracture Toughness Test

Fracture toughness tests were carried out on specimens with a notch (depth of 6 μm and notch radius of 0.25 μm) and those with a fatigue pre-crack (length of 3 μm) ahead of a notch (depth of 3 μm). In both the specimens, the total crack (or notch) length was adjusted to be $a/W \sim 0.5$. The notch position is the same as in the specimens for fatigue crack growth tests. Fracture toughness tests were also carried out using the mechanical testing machine for micro-sized specimens.

RESULTS AND DISCUSSION

Fatigue Crack Growth Behavior

Figure 3(a) shows a scanning electron micrograph of the specimen appearance after a fatigue crack growth test at a stress ratio of 0.5. A fatigue crack initiates from the notch root. The crack did not start to grow immediately after applying cyclic load and the crack started to grow after approximately 20,000 cycles (this was confirmed by a compliance change of the specimen during fatigue test). This indicates that even the notch with root radius of only 0.25 μm is not regarded as a natural crack for micro-sized specimens. Figure 3(b) shows a high magnification of the center region of the fracture surface. The upper part of Fig. 3(b) is a notch and the bottom region is a final fracture surface featured by a vein pattern which is observed on monotonic fracture surface in amorphous alloys [7]. The region between the notch and the final fractured region is thus a fatigue surface. The fatigue surface is relatively flat and very fine equispaced markings are clearly observed on the fatigue surface. The spacing between these markings are approximately 30 nm near the notch and 80 nm near the final fractured region, and increased with the crack extension. It is not certain whether these markings correspond to striations, but these markings are aligned perpendicular to the crack growth direction and were not observed on the

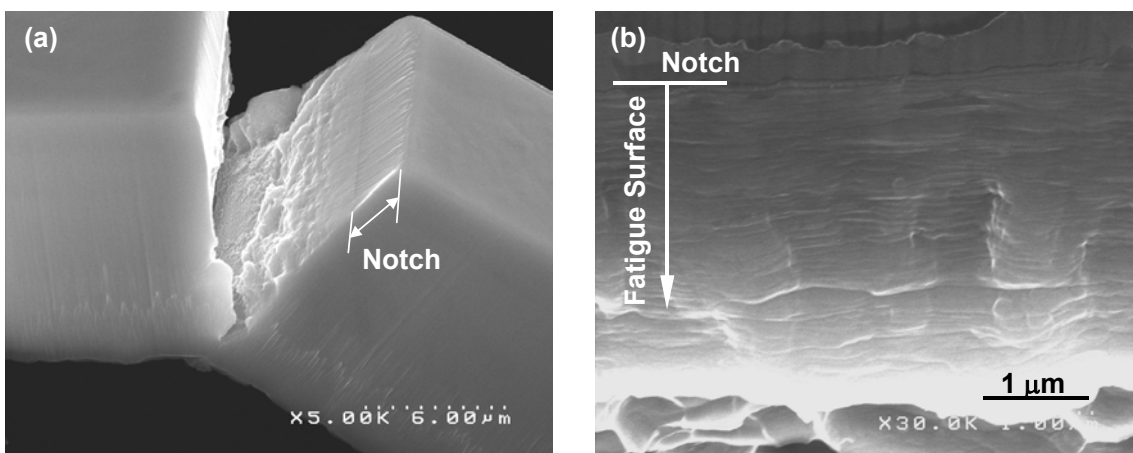


Figure 3: Scanning electron micrographs of micro-sized specimen after fatigue crack growth test. (a) close view near notch and fracture surface and (b) high magnification of fatigue surface.

fracture surface by static bending tests [8], so these markings are deduced to be striations. Such striations have also been observed on fatigue surfaces of metallic glass bulk specimens [9]. The formation of striations suggests that the crack has propagated by cyclic plastic deformation at the crack tip (i.e., blunting and resharping of crack tip). Actually, shear bands which are considered to be formed by plastic deformation were observed on the side surface of the specimen near the crack tip. Consequently, the fatigue crack growth seems to be based on cyclic plastic deformation at the crack tip even in micro-sized amorphous alloys.

If the spacing between the striations on the fatigue surface is assumed to be equivalent to the fatigue crack growth rate for the specimens, a fatigue crack growth resistance curve can be obtained from the measurement of the striation spacings. Careful measurements of the striation spacings were made and fatigue crack growth rates (da/dN) as a function of applied stress intensity factor range (ΔK) (where $\Delta K = K_{\max} - K_{\min}$) were obtained. Stress intensity factor (K) is calculated based on the equation obtained for a single edge notched cantilever beam specimen [10]. Figure 4 shows the fatigue crack growth resistance curve at a stress ratio of 0.5. As once a crack started to grow, the specimen failed after only several thousand cycles for the micro-sized specimens, so ΔK_{th} (a stress intensity range at which a crack starts to grow) was not able to be determined. Also, the number of data points is only three, but this is due to the difficulty in the measurement of striation spacings since the spacing is only between 20 - 70 nm. Therefore, It is not certain whether a Paris-Erdogan relationship ($da/dN = A\Delta K^m$, where A and m are material constants) is applicable for these data.

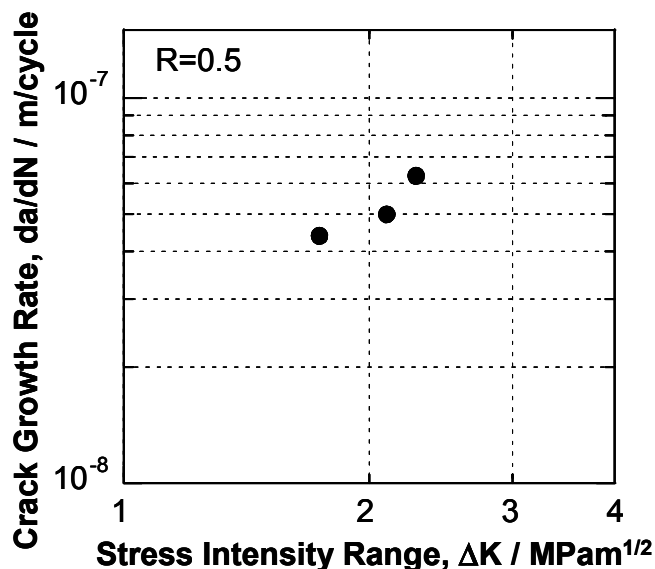


Figure 4: Fatigue crack growth resistance curve of micro-sized Ni-P amorphous alloy specimen.

The final fatigue fracture occurred at the crack growth rate less than 10^{-7} m/cycle. This crack growth rate is much lower compared to that of ordinary-sized specimens. This means that once a fatigue crack starts to grow then the fatigue fracture occurs only after several thousands of cycles. Therefore, the fatigue life of micro-sized specimens is mainly dominated by crack initiation. This also suggests that even micro-sized surface flaws may be an initiation site of fatigue crack growth and this will shorten the fatigue life of micro-sized specimens.

Fracture Toughness Tests

Figure 5 shows typical load - displacement curves for the specimens with a notch only and with a fatigue pre-crack. The fracture behavior is different between these two specimens. The specimen with a notch only fractured in a brittle manner, while the specimen with a fatigue pre-crack fractured in a ductile manner. The maximum load of the specimen with a notch only is approximately twice as that of the specimen with a fatigue pre-crack. This may be due to the difference in stress concentration at the crack

tip. The stress concentration arising at a fatigue crack tip is larger than that of the notch tip. This indicates that even the notch with a root radius of $0.25\ \mu\text{m}$ is not able to be regarded as a crack for micro-sized specimens. In addition, the ion implantation caused by focused ion beam machining may change the mechanical properties around the notch tip. As the depth of ion implantation area is estimated to be less than $1\ \mu\text{m}$, the influence of ion implantation can be ignored by introducing a fatigue pre-crack of more than $1\ \mu\text{m}$ in length. Therefore, it is essential for evaluating fracture toughness to introduce a fatigue pre-crack for the material used in this investigation.

Figure 6 shows a scanning electron micrograph of fracture surface of the specimen with a fatigue pre-crack. The slant fractured regions which appear to be shear lips are clearly observed near the side surfaces of the crack. The width of the region is approximately $3\ \mu\text{m}$. If these are shear lips, these areas should be plane stress dominated regions. The width of shear lip is expressed approximately as $2r_y/3$, where r_y is the size of plane stress plastic zone ($r_y = (K/\sigma_y)^2/\pi$, where K is the stress intensity factor and σ_y is the yield stress of the specimen) [11]. The calculated value of shear lip width at the maximum load is $2.8\ \mu\text{m}$ (the value of $\sigma_y = 2.0\ \text{GPa}$ in this amorphous alloy thin film was quoted [12] in this calculation). These sizes are very close to the those of slant fractured regions in Fig. 6. Therefore,

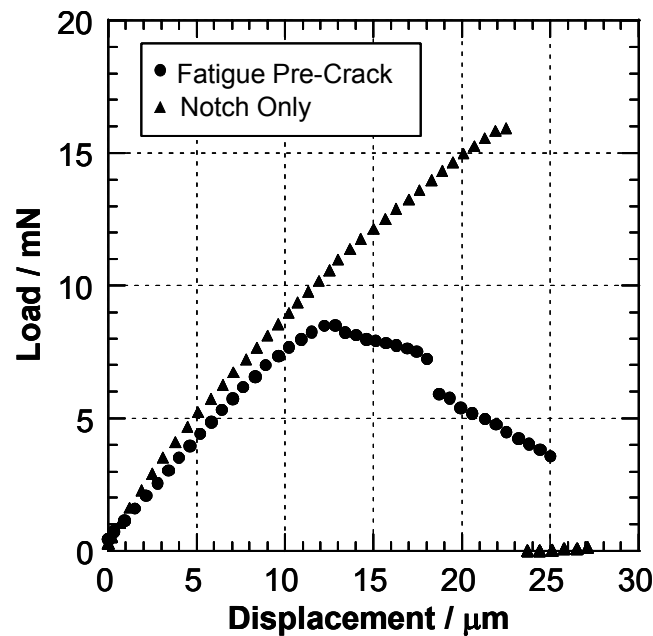


Figure 5: Load-displacement curves for micro-sized specimens with a notch only and with a fatigue pre-crack.

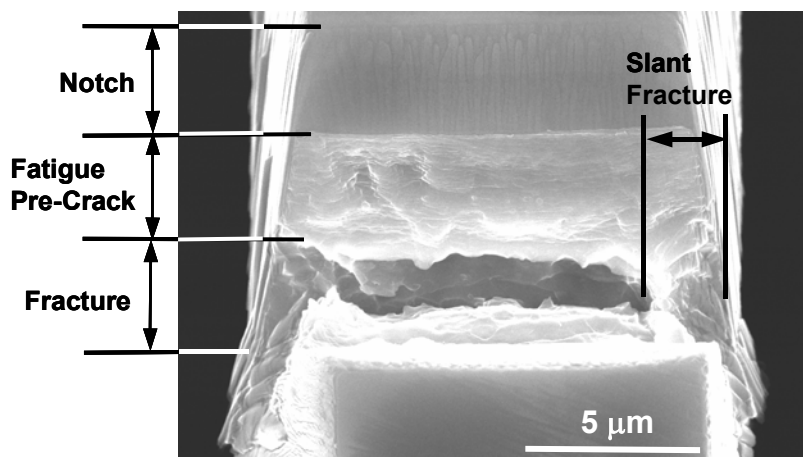


Figure 6: Scanning electron micrograph of fracture surface.

these slant fractured zones are plane stress dominated region and the flat region corresponds to plane strain dominated one. It is very interesting to note that there exists a plane strain region even in such micro-sized specimens.

As crack opening displacement was not able to be measured for this specimen, the crack initiation load was not able to be determined. The maximum load was then assumed to be the crack initiation load and this load was used to calculate a fracture toughness value. The total pre-crack length was measured from Fig. 6. The calculated provisional fracture toughness values (K_Q) for the specimen with fatigue pre-crack is $7.3 \text{ MPam}^{1/2}$. However, this value is not a valid plane strain fracture toughness values (K_{IC}), as the criteria of plane strain requirements ($a, W-a, B > 2.5 (K_Q/\sigma_y)^2$) were not satisfied for this specimen size. As the plane strain requirements are determined by K and σ_y , it is difficult for micro-sized specimens to satisfy these requirements. Consequently, another criterion such as J integral might be required to evaluate fracture toughness of such micro-sized specimens.

CONCLUSIONS

Fatigue crack growth and fracture toughness tests have been performed on micro-sized Ni-P amorphous alloy specimens. Once fatigue crack growth occurs, the specimens failed after several thousand cycles. This indicates that the fatigue life of micro-sized specimens is dominated by crack initiation. This also suggests that even a micro-sized surface flaw may be an initiation site of fatigue crack and this will shorten the fatigue life of micro-sized specimens. It is essential for evaluating fracture toughness to introduce a fatigue pre-crack even for micro-sized specimens. The plane strain fracture toughness, K_{IC} , value was not obtained since the criteria of plane strain were not satisfied for this size of specimens. As the plane strain requirements are determined by stress intensity and yield stress of the material, it is rather difficult for micro-sized specimens to satisfy these requirements. Plane stress and plane strain dominated regions were clearly observed on the fracture surfaces and their sizes were consistent with those estimated by fracture mechanics calculations.

REFERENCES

1. Shrape, Jr., W. N., Yuan, B. and Edwards, R. L. (1997) *J. Microelectromechanical Systems*, **6**, 193.
2. Ballarini, R., Mullen, R. L., Yin, Y., Kahn, H., Stemmer, S. and Heuer, A. H. (1997) *J. Mater. Res.* **12**, 915.
3. Sato, K., Yoshioka, T., Ando, T., Shikada, M. and Kawabata, T. (1998) *Sensors and Actuators A: Physical*, **70**, 148.
4. Takashima, K., Kimura, T., Shimojo, M., Higo, Y., Sugiura, S. and Swain, M. V. (1999). In: *Fatigue '99 (Proc. 7th Int. Fatigue Cong.)*, pp. 1871-1876, Wu, X-R. and Wang, Z-G., (Eds). Higher Education Press, Beijing.
5. Higo, Y., Takashima, K., Shimojo, M., Sugiura, S., Pfister, B. and Swain, M. V. (2000). In: *Materials Science of Microelectromechanical Systems (MEMS) Devices II*, pp. 241-246, deBoer, M. P., Heuer, A. H., Jacobs, S. J. and Peeters, E., (Eds). The Materials Research Society, Pennsylvania.
6. Maekawa, S., Takashima, K., Shimojo, M., Higo, Y., Sugiura, S., Pfister, B. and Swain, M. V. (1999) *Jpn. J. Appl. Phys.*, **38**, 7194.
7. Misknf, J., Csach, K., Ocelik, V. and Duhaj, P. (1997) *Mat. Sci. Eng.*, **A226-228**, 883.
8. Ichikawa, Y., Maekawa, S., Takashima, K., Shimojo, M., Higo, Y. and Swain, M. V. (2000). In: *Materials Science of Microelectromechanical Systems (MEMS) Devices II*, pp. 273-278, deBoer, M. P., Heuer, A. H., Jacobs, S. J. and Peeters, E., (Eds). The Materials Research Society, Pennsylvania.
9. Gilbert, C. J. and Ritchie, R. O. (1997) *Appl. Phys. Lett.*, **71**, 476.
10. Okamura, H. (1976). *Introduction to Linear Fracture Mechanics*, Baifukan, Tokyo, (in Japanese).
11. Knott, J. F. (1976). *Fundamentals of Fracture Mechanics*, Butterworths, London.
12. Morita, A., Takashima, K. and Higo, Y., to be published.